







# Ultrasonic Cleaning of Ore Particles and Disintegration of Flocculation Formations

Vladimir Morkun<sup>1</sup><sup>a</sup>, Natalia Morkun<sup>1</sup><sup>b</sup>, Vitalii Tron<sup>2</sup><sup>c</sup>, Oleksandra Serdiuk<sup>2</sup><sup>d</sup>,  
Iryna Haponenko<sup>3</sup><sup>e</sup> and Alona Haponenko<sup>3</sup><sup>f</sup>

<sup>1</sup>Faculty of Engineering Sciences, Bayreuth University, Universitätsstraße, 30, Bayreuth, 95447, Germany

<sup>2</sup>Department of Automation, Computer Science and Technology, Kryvyi Rih National University,  
11 Vitalii Matusevych Str., Kryvyi Rih, 50027, Ukraine

<sup>3</sup>Research Department, Kryvyi Rih National University,  
11 Vitalii Matusevych Str., Kryvyi Rih, 50027, Ukraine

**Keywords:** Ultrasonic Cleaning, Ore Particles, Disintegration, Flocculation, Ore Processing.

**Abstract:** The research is aimed at increasing efficiency of magnetite concentrate flotation by cleaning the surface of useful component particles through disintegrating ore flocculated formations. The generalized model of bubble motion dynamics with time-dependent pressure and bubble size is presented. Computer modelling of bubbles behaviour under the action of ultrasonic radiation is performed. The high-energy ultrasound power is calculated to maintain cavitation modes in the iron ore slurry. The research into flocculation and deflocculation considers the dependence of magnetic susceptibility on duration of magnetization. The modelling results enable the conclusion that in order to improve quality of cleaning ore particles before flotation, it is advisable to apply a spatial effect to the iron ore slurry by means of high-energy ultrasound of 20 kHz in the cavitation mode modulated by high-frequency pulses of 1 MHz to 5 MHz.

## 1 INTRODUCTION


In the liquid medium, some physical, chemical and physicochemical processes occur including cavitation, radiation pressure and ultrasonic flows under the influence of ultrasound (Gubin et al., 2017; Morkun et al., 2014). Since liquids are sensitive to stretching forces, therefore, under powerful ultrasonic oscillations, compression and liquefaction zones arise in the liquid. During the wave phase, which creates liquefaction, there are many gaps in the form of cavitation bubbles in the liquid, which close abruptly in the subsequent phase of compression.


Different effects of ultrasound on individual minerals, are used to achieve high dispersion (Soyama and Korsunsky, 2022; Golik et al., 2015; Morkun et al., 2017), for example, for grinding schistose min-


erals (graphite, molybdenite). The process of grinding molybdenite under excessive static pressure results in manufacturing a product, the dispersion of which is 2-3 times higher than that of the product obtained under atmospheric pressure (Soyama and Korsunsky, 2022).


Application of ultrasound to processing ore raw materials has been an urgent research problem for a long time. In particular, introduction of ultrasound into the water system of ore processing provides specific activation based on two physical phenomena – acoustic cavitation and acoustic wind (Ambedkar et al., 2011; Ambedkar, 2012; Morkun et al., 2015a; Morkun and Morkun, 2018). Gas discharge in acoustic cavitation is most preferable at lower frequency within 20kHz-40kHz, while the acoustic wind dominates at frequencies above 400kHz and 1MHz in ultrasonic and megasonic systems, respectively (Ambedkar et al., 2011).


The experiment results in (Harrison et al., 2002) reveal an increase in the clean coal yield from 3 % to 10 %, greater production of clean coal and a decrease in the content of sulfur, mercury, ash and moisture in the processed coal. These results are associated with


<sup>a</sup> <https://orcid.org/0000-0003-1506-9759>

<sup>b</sup> <https://orcid.org/0000-0002-1261-1170>

<sup>c</sup> <https://orcid.org/0000-0002-6149-5794>

<sup>d</sup> <https://orcid.org/0000-0003-1244-7689>

<sup>e</sup> <https://orcid.org/0000-0002-0339-4581>

<sup>f</sup> <https://orcid.org/0000-0003-1128-5163>

ultrasonic shock waves generated by bubble cavitation that contributes to breaking natural relationships between coal and ash-forming mineral impurities and cleaning of coal particles from impurities. Cavitation also enhances removal of unwanted particles of clay, slime and oxidation products covering the surface of coal.

Application of the above methods is a promising approach to improving efficiency of technological processes of iron ore beneficiation (Morkun et al., 2015b,c).

The research aims to increase efficiency of flotation of magnetite concentrates by disintegrating ore flocculated formations and cleaning particle surfaces. To achieve the set aim, it is necessary to investigate peculiarities of formation of cavitation modes in iron ore slurry by applying high-energy ultrasound.

## 2 MATERIALS AND METHODS

Let us consider mathematical description of cavitation processes in the heterogeneous medium. The generalized model of bubble motion dynamics dependent on the pressure time and the size of bubbles is presented as a Rayleigh-Plesset equation (Gubin et al., 2017; Kozubková et al., 2012). Solving the Rayleigh-Plesset equation for a certain pressure value  $p_\infty(t)$  enables obtaining the value of the bubble radius  $dR_b(t)$

$$\frac{dR_b}{dt} = \sqrt{\frac{2}{3} \frac{p_{vap}(t) - p_\infty(t)}{\rho_1}}, \quad (1)$$

where  $R_b$  is the bubble radius,  $\mu\text{m}$ ;  $p_\infty$  is pressure in the medium at perpetuity, Pa;  $p_{vap}$  is vapour pressure, Pa;  $\rho_1$  is liquid density,  $\text{kg}/\text{m}^3$ .

The results of Singhal et al. (Singhal et al., 2002) suggests a cavitation model based on a complete cavitation model. The density of the mixture is defined as

$$\rho = \alpha \rho_{vap} + (1 - \alpha) \rho_1, \quad (2)$$

where  $\alpha$  is the volumetric fraction of vapour;  $\rho_{vap}$  is vapour density,  $\text{kg}/\text{m}^3$ ;  $\rho_1$  is liquid density,  $\text{kg}/\text{m}^3$ . The ratio between density of the mixture and the volumetric fraction of vapour  $\alpha$  has the form:

$$\frac{\partial}{\partial t}(\rho) = -(\rho_1 - \rho_{vap}) \frac{\partial}{\partial t}(\alpha), \quad (3)$$

where  $\rho$  is density of the mixture,  $\text{kg}/\text{m}^3$ ;  $\alpha$  is the volumetric fraction of vapour;  $\rho_{vap}$  is vapour density,  $\text{kg}/\text{m}^3$ ;  $\rho_1$  is liquid density,  $\text{kg}/\text{m}^3$ . The volumetric fraction of vapour  $\alpha$  is determined from  $f$  as

$$\alpha = f \frac{\rho}{\rho_{vap}}. \quad (4)$$

According to the cavitation model proposed in (Schnerr and Sauer, 2001), the equation for the particle volumetric fraction of vapour  $\alpha$  is obtained from the expression

$$R = \frac{\partial}{\partial t}(\rho_{vap} \alpha) + \frac{\partial}{\partial x_j}(\rho_{vap} \alpha \bar{u}_j), \quad (5)$$

where  $R$  is the evaporation rate,  $\text{kg}/\text{h}$ .

$$R = \frac{\rho_{vap} \rho_1}{\rho} \left( \frac{\partial \alpha}{\partial t} + \frac{\partial (u_j \alpha)}{\partial x_j} \right) \quad (6)$$

When substituting equation (5) in (6) we obtain

$$R = \frac{\rho_{vap} \rho_1}{\rho} \alpha (1 - \alpha) \frac{3}{R_b} \sqrt{\frac{2}{3} \frac{(p_{vap} - p)}{\rho_1}} \quad (7)$$

The bubble radius is determined from the expression

$$R_b = \left( \frac{\alpha}{1 - \alpha} \frac{3}{4\pi n_b} \right)^{\frac{1}{3}}. \quad (8)$$

Also in this model, the only parameter to be determined is the number of spherical bubbles in the volume of liquid  $n_b$ .

Equation (7) is also used to simulate the condensation process. The final form of the model is as follows:

if  $p \leq p_{vap}$

$$R_e = \frac{\rho_v \rho_1}{\rho} \alpha (1 - \alpha) \frac{3}{R_b} \sqrt{\frac{2}{3} \frac{(p_{vap} - p)}{\rho_1}}. \quad (9)$$

if  $p \geq p_{vap}$

$$R_c = \frac{\rho_v \rho_1}{\rho} \alpha (1 - \alpha) \frac{3}{R_b} \sqrt{\frac{2}{3} \frac{(p - p_{vap})}{\rho_1}}. \quad (10)$$

If ultrasonic frequency is small ( $< 1\text{MHz}$ ) and pressure amplitude is much smaller than the atmospheric static pressure (101 kPa), a bubble will be in the state of stable cavitation (Hu, 2013), i.e. fluctuate around its initial radius in the periodic mode periodically. This process should be described using an empirical equation based on the simplified Keller-Herring model (Carvell and Bigelow, 2011)

$$R_0 \cong 3 \{MHz\} \frac{\mu m}{f_0^{lin}}, \quad (11)$$

where  $R_0$  is the radius of the bubble,  $\mu\text{m}$ ;  $\mu$  is the shearing viscosity coefficient,  $f_0^{lin}$  is ultrasonic frequency, MHz.

It should be noted that at higher pressure, the bubble reaction also largely depends on the ultrasonic field pressure amplitude and, therefore, equation (11) is no longer possible in this ‘‘inertial cavitation’’ scenario.

There are expressions in (Carvell and Bigelow, 2011) to calculate the optimal initial radius of the bubble for maximum expansion depending on ultrasonic frequency and pressure amplitude

$$R_{optimal} = \frac{1}{\sqrt{0.0327F^2 + 0.0679F + 16.5P^2}}, \quad (12)$$

where  $P$  is the pressure amplitude for the ultrasonic sinusoidal wave, MPa;  $f$  is frequency, MHz;  $R_{optimal}$  is the optimal bubble radius,  $\mu\text{m}$ .

For example, if  $f = 1\text{MHz}$ ,  $P = 1\text{MPa}$ , the optimal bubble radius is  $0.2454\text{m}$ .

Calculation covers the frequency range, MHz, pressure amplitudes, MPa and radii,  $\mu\text{m}$  used in modelling (Hu, 2013) (table 1). It should be noted that at  $f = 0.5\text{MHz}$  and pressure  $P = 8.0\text{MPa}$  the initial radius is  $R = 30.75\text{nm}$ .

After converting dependence (12), we get a square equation that includes the function of optimal frequency for a certain size of bubbles from where  $F(R)$  at the known pressure  $P$  can be determined from the expression

$$F(R) = \frac{-0.068 \pm \sqrt{0.068^2 - 4 \cdot 0.034 \cdot (6.5P^2 - \frac{1}{R})}}{2 \cdot 0.033}. \quad (13)$$

where  $R_{optimal}$  is the optimal bubble size,  $\mu\text{m}$ ;  $F()$  is frequency of high-energy ultrasound, MHz.

Consequently, the cavitation mode with the known bubble size is formed by impacting the slurry with high-energy ultrasound with  $F(R_{optimal})$  frequency.

We denote the function of distributing bubbles by size by  $f(R)$ , then the value  $f(R)dR$  determines the fraction of bubbles within the size range of  $R$  to  $R + dR$ .

Table 2 demonstrates the value of the function used in calculations.

The obtained dependences allow determining optimal frequency of high-energy ultrasound to maintain cavitation in the iron ore slurry depending on parameters of its components. Therefore, to form controlled cavitation processes and acoustic flows in the iron ore slurry, it is necessary to model dynamic effects of high-energy ultrasound in the heterogeneous medium.

### 3 RESULTS AND DISCUSSION

Bubble behavior under the influence of ultrasonic radiation is modelled by using a specialized software package Bubblesim in MATLAB (Hoff et al., 2000).

Dynamics of air bubble sizes during the modelling process is determined through the modified Rayleigh-Plesset equation (Hoff, 2001):

$$\ddot{a}a + \frac{3}{2}\dot{a}^2 + \frac{p_0 + p_i(t)p_L}{\rho} - \frac{a}{\rho c} \dot{p}_L = 0 \quad (14)$$

where  $a$  is the bubble radius, m;  $p_0$  is hydrostatic pressure, Pa;  $p_i$  is acoustic pressure, Pa;  $p_L$  is pressure on the bubble surface, Pa;  $\rho$  is fluid density,  $\text{kg/m}^3$ ;  $c$  is the sound speed, m/s.

The following dependence is used to determine the value of the bubble surface pressure  $p_L$ :

$$p_L = -4\eta_L \frac{\dot{a}}{a} - (T_2 - T_1) + p_g \left(\frac{a_e}{a}\right)^{3k} \quad (15)$$

where  $\eta_L$  is the internal friction coefficient;  $T_1$ ,  $T_2$  are tension of the inner and outer bubble walls, respectively;  $p_g$  is internal pressure of gas bubbles, Pa;  $k$  is the gas constant of the polytropic process.

The modelling results with nonlinear effects of high-energy ultrasound considered are presented in (figure 1): the driving pulse (figure 1, a), changes of the bubble radius (figure 1, b), the signal spectrum (figure 1, c).

During the study, the radiation pressure amplitude is  $0.3\text{MPa}$ , while the ultrasound frequency changes and makes  $1\text{MHz}$ ,  $3\text{MHz}$ ,  $5\text{MHz}$ .

To model the process of ultrasonic signal propagation in the liquid medium when changing the sound propagation rate and density, the 1st and 2nd-order k-space method is used based on the 1st-order linear equations (Tabei et al., 2002; Mast et al., 2001).

To apply the k-space method to the system of the 1st-order equations describing wave propagation, the 2nd-order k-space operator can be used by dividing it into parts associated with each spatial direction. For a two-dimensional case, this procedure is performed as follows

$$\frac{\partial p(r,t)}{\partial (c_0 \Delta t)_x^+} \equiv F^{-1} \left( ik_x e^{ik_x \Delta x / 2} \frac{\sin(c_0 \Delta t k / 2)}{c_0 \Delta t k / 2} F(p(r,t)) \right); \quad (16)$$

$$\frac{\partial p(r,t)}{\partial (c_0 \Delta t)_y^+} \equiv F^{-1} \left( ik_y e^{ik_y \Delta y / 2} \frac{\sin(c_0 \Delta t k / 2)}{c_0 \Delta t k / 2} F(p(r,t)) \right);$$

$$\frac{\partial p(r,t)}{\partial (c_0 \Delta t)_x^-} \equiv F^{-1} \left( ik_x e^{ik_x \Delta x / 2} \frac{\sin(c_0 \Delta t k / 2)}{c_0 \Delta t k / 2} F(p(r,t)) \right);$$

$$\frac{\partial p(r,t)}{\partial (c_0 \Delta t)_y^-} \equiv F^{-1} \left( ik_y e^{ik_y \Delta y / 2} \frac{\sin(c_0 \Delta t k / 2)}{c_0 \Delta t k / 2} F(p(r,t)) \right);$$

Table 1: Parameters of ultrasonic cavitation modes.

f, MHz	P, MPa								
	0.01	0.1	0.3	0.5	0.7	1.0	3.0	5.0	8.0
0.5	4.779	2.197	0.809	0.489	0.350	0.245	0.082	0.049	0.031
1.0	3.127	1.940	0.794	0.486	0.349	0.245	0.082	0.049	0.031
3.0	1.414	1.228	0.710	0.465	0.341	0.242	0.081	0.049	0.031
5.0	0.929	0.869	0.615	0.435	0.328	0.238	0.081	0.049	0.031

Table 2: Values of the function of distributing bubbles by size.

$R, m \times 10^{-6}$	3	5	10	20	50
$f(R), m^{-1}$	0.0054	0.0273	0.0545	0.330	0.545
$R, m \times 10^{-4}$	1.5	2.0	2.5	3.0	3.5
$f(R), m^{-1} \times 10^{-3}$	49	21.2	10.9	6.5	4.1

so that

$$\left( \frac{\partial p(r,t)}{\partial (c_0 \Delta t)^+ x} \frac{\partial p(r,t)}{\partial (c_0 \Delta t)^- x} + \frac{\partial p(r,t)}{\partial (c_0 \Delta t)^+ y} \frac{\partial p(r,t)}{\partial (c_0 \Delta t)^- y} \right) p(r,t) = \left( \nabla^{(c_0 \Delta t)} \right)^2 p(r,t) \quad (17)$$

Spatial-frequency components  $k_x$  and  $k_y$  are determined so that  $k^2 = k_x^2 + k_y^2$ . The use of equation operators (16) in (15) enables formation of the 1st-order k-space method which is equivalent to equation (14). Application of exponential coefficients from equation (16) requires evaluation of ultrasonic wave velocities  $u_x$  and  $u_y$  at the grid points at intervals  $\Delta x/2$  and  $\Delta y/2$ , respectively. The resulting algorithm has the form

$$\begin{aligned} \frac{u_x(r_1, t^+) - u_x(r_1, t^-)}{\Delta t} &= \frac{1}{\rho(r_1)} \frac{\partial p(r,t)}{\partial (c_0 \Delta t)^+ x}; \\ \frac{u_y(r_2, t^+) - u_y(r_2, t^-)}{\Delta t} &= \frac{1}{\rho(r_2)} \frac{\partial p(r,t)}{\partial (c_0 \Delta t)^+ y}; \\ \frac{p(r, t + \Delta t) - p(r, t)}{\Delta t} &= \\ &= -\rho(r) c(r)^2 \left( \frac{\partial u_x(r_1, t^+)}{\partial (c_0 \Delta t)^- x} + \frac{\partial u_y(r_2, t^+)}{\partial (c_0 \Delta t)^- y} \right) \end{aligned} \quad (18)$$

where

$$\begin{aligned} r_1 &\equiv (x + \Delta x/2, y), \quad r_2 \equiv (x, y + \Delta x/2), \\ t^+ &\equiv t + \Delta t/2, \quad t^- \equiv t - \Delta t/2. \end{aligned} \quad (19)$$

In equation (18), the coefficients  $c_0$  and  $\rho_0$  are replaced spatially and transformed by values of the sound speed and density  $c(r)$  and  $\rho(r)$ . Spatial distribution in equation (18) is implicitly introduced into spatial derivatives of the operators considered. For example, operators

$$\partial / \partial (c_0 \Delta t)^+ x$$

and

$$\partial / \partial (c_0 \Delta t)^- x$$

determined by formula (16) correspond to derivatives calculated after spatial shifts according to the Fourier transformation shift property  $\Delta x/2$  and  $-\Delta x/2$ , respectively.

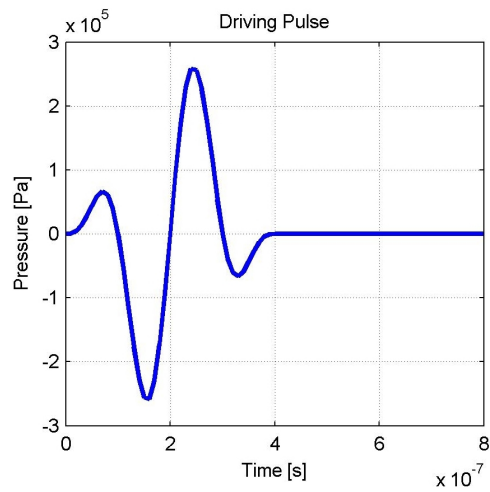
High-energy ultrasound power, which allows maintaining cavitation modes in the iron ore slurry, is calculated on the basis of the above results of studying distribution of the ultrasonic pulse front by using HI-FUSimulator v1.2 (Soneson, 2011). The calculation results are given in figures 3, 4, 5, 6, 7.

The modelling results enable us to conclude that in order to improve quality of cleaning ore particles before flotation, it is advisable to apply a spatial effect to the iron ore slurry by means of high-energy ultrasound of 20kHz in the cavitation mode modulated by high-frequency pulses of 1 MHz - 5 MHz.

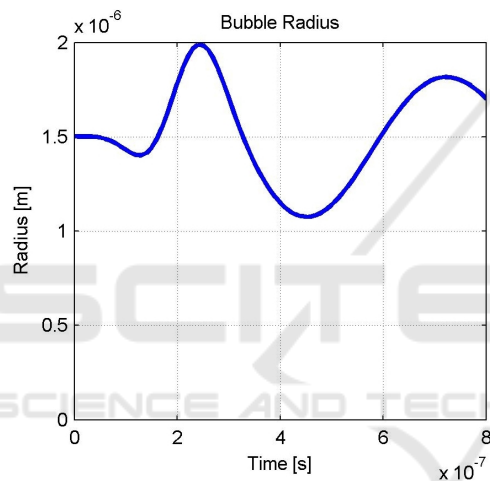
At the same time, the reasons for forming flocs from particles of magnetite iron ore slurry, which being beneficiated move relative to each other and interact with their poles, include movement of ferromagnetic particles in the magnetic field to reduce total magnetostatic energy (energy of free poles) (Karmazin and Karmazin, 2005). This phenomenon is an integral part of beneficiation of fine materials with significant magnetic properties and directly affects efficiency of beneficiation. The size of flocs can vary from 2 to 1000 diameters of the particles forming them.

The phenomenon of fluctuations of monopolar blast furnace boundaries under the action of ultrasonic waves propagating along them is explained by the fact that ultrasound causes variable mechanical stresses in iron particles, which leads to an increase in magnitude of magneto-elastic energy  $U_d$  generally determined from the expression (Vlasko-Vlasov and Tikhomirov, 1991)

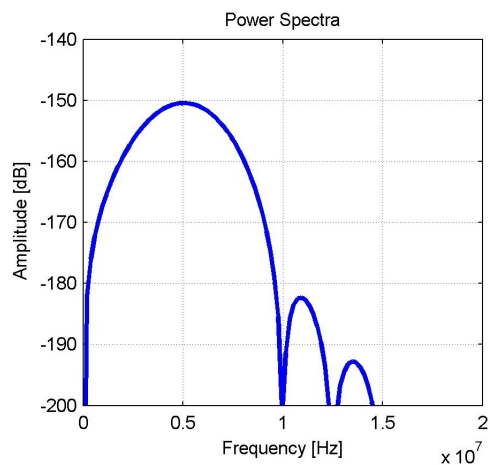
$$U_d = -\sigma \cdot \lambda \quad (20)$$



(a)



(b)



(c)

Figure 1: Modelling results of cavitation processes under high-energy ultrasound.

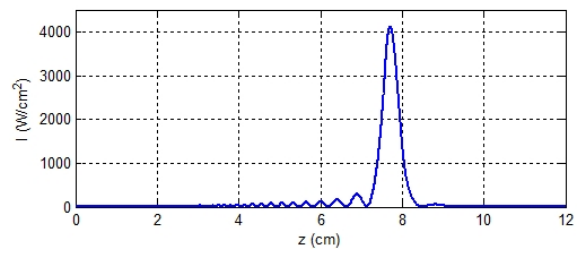


Figure 2: Radial intensity in the ultrasound focus.

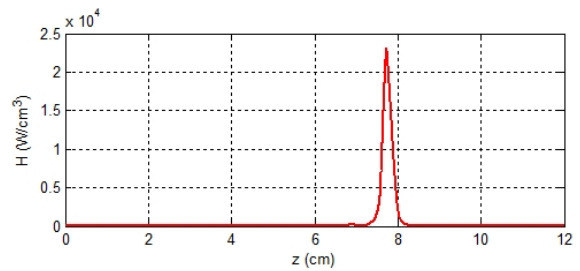


Figure 3: Intensity in the ultrasound focus.

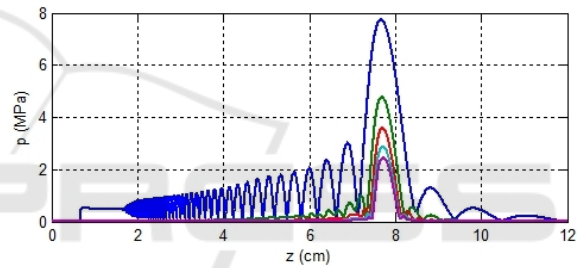


Figure 4: Axial distribution of pressure of the first five harmonics of ultrasonic radiation.

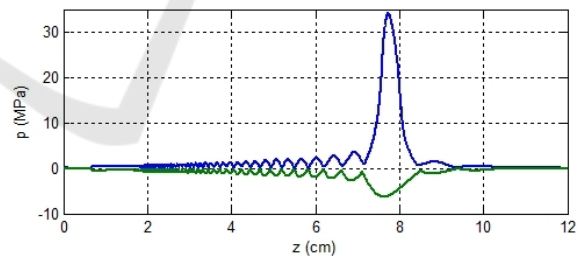


Figure 5: Axial pressure peaks in ultrasonic radiation.

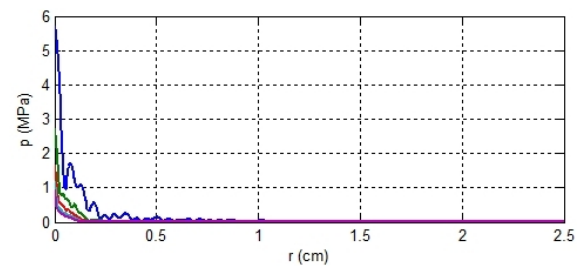


Figure 6: Distribution of radial pressure of the first five harmonics in the ultrasonic radiation focus.

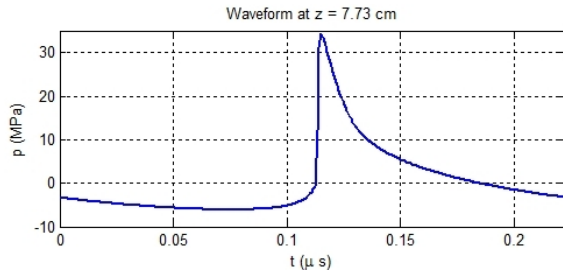


Figure 7: Shape of the ultrasonic wave along the radiation axis at the distance ( $z=7.73$  cm), which corresponds to the peak intensity.

where  $\lambda$  is magnetostriction;  $\sigma$  is tension.

According to the Akulov anisotropy law, the expression for  $U_d$  has the following form (Chikazumi, 2009):

$$U_d = -\sigma \cdot \left( a_1 \sum_{i=1,2,3} \left( S_i^2 \beta_i^2 - \frac{1}{3} \right) + a_2 \sum_{i \neq j} (S_i S_j \beta_i \beta_j) \right) \quad (21)$$

To observe the condition

$$\frac{\partial (U_K + U_D + U_H)}{\partial \alpha} = 0 \quad (22)$$

where  $U_K$  is magnetic anisotropy energy of a crystal;  $U_H$  is energy of the external magnetic field.

According to expressions (20)–(22), if energy  $U_H$  changes, magnetism of the particles increases.

Interaction of magnetic masses in flocculation is described in accordance with the Coulomb law to determine the strength of flocculated formations  $F_{fl}$  (Karmazin and Karmazin, 2005):

$$F_{fl} = \sigma_{fl} S = k \chi^2 H^2 s^2 / (\mu_0 r^2) \quad (23)$$

where  $\sigma_{fl}$  is the floccule strength,  $S$  is the area of the floccule cross section,  $k$  is the coefficient specifying the coordinate of the point of magnetic mass concentration,  $\xi$  is magnetic susceptibility,  $H$  is intensity of the magnetic field,  $r$  is the distance of interaction.

The strength of floccules is determined by the expression (Karmazin and Karmazin, 2005):

$$\sigma_{fl} = k J^2 / (1 - \chi N)^2 \quad (24)$$

where  $k$  is the proportionality coefficient;  $J$  is floccule magnetization;  $N$  is the floccule demagnetization coefficient. This characteristic is also evaluated by the expression of ferromagnetic energy:

$$F_{fl} = -\frac{dU}{dx} = -\frac{d(BHV)}{dx} = -0.5 BHV = -0.5 \mu H^2 s; \quad \sigma_{fl} = 0.5 \mu H^2. \quad (25)$$

When studying flocculation and deflocculation, one should consider the dependence of magnetic susceptibility  $\gamma_c$  on duration of magnetization  $t$ .

The dependence of the flocculation degree  $\Psi$  and the field intensity looks like (Karmazin and Karmazin, 2005):

$$\Psi = k_1 H_0^2 + \Delta \Psi \delta(H - H_{kr}) + (1 + \Psi_2) (1 - \exp(-k_2 (H - H_{kr}))), \quad (26)$$

where  $H_0$  is initial intensity of the magnetic field which causes equilibrable reversible flocculation;  $\Delta \Psi = \Psi_1 - \Psi_2$  is an increase in the flocculation degree due to the avalanche process;  $\Psi_1 - \Psi_2$  are flocculation degrees at the beginning and at the end of the avalanche process, respectively, which are functions of concentration, the formfactor, size and magnetic susceptibility of flocculating particles;  $H_{kr}$  is critical field tension causing avalanche flocculation  $H_0 < H_{kr}$ ;  $k_1$ ,  $k_2$  are intensity coefficients presented as functions of concentration, magnetic susceptibility, the formfactor, the Reynolds parameter for the hydromechanical mode of the medium motion, particle size dependent on time [ $k_2 = f(C, N, \kappa, Re, d, t)$ ];  $\delta(H - H_{kr})$  is the Dirac function from tension;  $\int_{H_{kr}-\Delta}^{H_{kr}+\Delta} \delta(H - H_{kr}) dH = 1$ , where  $\Delta$  is a small number.

The dependence of size of the narrow fraction particle extracted from the floccule (flocculation degree)  $E$  obtained in (Karmazin and Karmazin, 2005; Chikazumi, 2009), shows a significant dependence of flocculation on the content of the ferromagnetic component in the iron ore slurry:

$$E = 1 - e \left( \frac{r_0 v_0 t}{\int_{r_0}^{R_f} \exp(-k \chi d (r_0^{-1} - r^{-1}) / (3\pi \mu D_t)) r dr} \right) \quad (27)$$

nonident where  $r_0$  is the radius of the floccule;  $v_0$  is the speed of particles of a narrow fraction near the surface of the floccule;  $t$  is flocculation time;  $D_t$  is the turbulent diffusion coefficient. It should be noted that with decreased size, magnetic susceptibility of the magnetic sharply decreases, and the coercive force increases sharply, which is explained by approximation to the monodomain size of magnetite, that complicating the flocculation process.

When implementing this approach, the ultrasonic wave radiator should be able to vary frequency during measurements in a fairly wide range. In practice, this can be done by means of the ultrasonic phased array. While developing its design, the influence of the distance between elements, wavelength and the number of elements on controllability and efficiency of ultrasonic radiation are investigated. Optimal parameters of the ultrasonic phased array are selected by indicators that characterize its directional diagram (Morkun et al., 2015b,c).

Analysis of the research results enables concluding that in order to increase efficiency of the flotation

process by disintegrating flocculated ore formations, it is advisable to exert a spatial effect on the iron ore slurry including a combination of high-energy ultrasound and the pulsed magnetic field of descending intensity.

The modelling results enable concluding that to improve quality of ore particles cleaning before flotation, it is advisable to apply a spatial effect to the iron ore slurry. This includes a combination of high-energy ultrasound of 20 kHz in the cavitation mode modulated by high-frequency pulses within 1 MHz-5 MHz and the pulsed magnetic field of descending intensity. The next stage involves calculation of characteristics of these effects and determination of the device parameters to disintegrate flocculated ore formations in the slurry flow on the basis of the ultrasonic phased array.

## 4 CONCLUSIONS

To increase efficiency of magnetite concentrates flotation by disintegrating flocculated ore formations and cleaning the particle surface, it is advisable to use nonlinear effects of the high-energy ultrasonic field to form and maintain cavitation processes and acoustic flows in the iron ore slurry.

Investigation into cavitation patterns results in dependences obtained to determine optimal frequency of high-energy ultrasound aimed to maintain cavitation processes in the iron ore slurry depending on parameters of its components.

Based on the modelling results, it is established that in order to improve quality of ore particles cleaning before flotation, a spatial effect should be exerted on the iron ore slurry, which includes a combination of 20kHz high-energy ultrasound in the cavitation mode modulated by high-frequency pulses of 1 MHz-5 MHz and the pulsed magnetic field of descending intensity.

## REFERENCES

- Ambedkar, B. (2012). *Ultrasonic Coal-Wash for De-Ashing and De-Sulfurization: Experimental Investigation and Mechanistic Modeling*. Springer Theses. Springer Berlin, Heidelberg. <https://doi.org/10.1007/978-3-642-25017-0>.
- Ambedkar, B., Nagarajan, R., and Jayanti, S. (2011). Investigation of High-Frequency, High-Intensity Ultrasonics for Size Reduction and Washing of Coal in Aqueous Medium. *Ind. Eng. Chem. Res.*, 50(23):13210–13219. <https://doi.org/10.1021/ie200222w>.
- Carvell, K. J. and Bigelow, T. A. (2011). Dependence of optimal seed bubble size on pressure amplitude at therapeutic pressure levels. *Ultrasonics*, 51(2):115–122. <https://doi.org/10.1016/j.ultras.2010.06.005>.
- Chikazumi, S. (2009). *Physics of Ferromagnetism*, volume 94 of *International Series of Monographs on Physics*. Oxford University Press, Oxford, 2 edition.
- Golik, V., Komashchenko, V., Morkun, V., and Zaalishvili, V. (2015). Enhancement of lost ore production efficiency by usage of canopies. *Metallurgical and Mining Industry*, 7(4):325–329. [https://www.metaljournal.com.ua/assets/MML\\_2014\\_6/MML\\_2015\\_4/047-GolikKomashchenkoMorkunZaalishvili.pdf](https://www.metaljournal.com.ua/assets/MML_2014_6/MML_2015_4/047-GolikKomashchenkoMorkunZaalishvili.pdf).
- Gubin, G. V., Tkach, V. V., and Ravinskaya, V. O. (2017). Application of ultrasound for cleaning the surface of altered mineral particles before flotation [Primene-nie ul'trazvuka dlja ochistki poverhnosti izmenennykh mineral'nykh chastic pered flotaciej]. *The quality of mineral raw materials*, 1:341–349.
- Harrison, C. D., Raleigh, Jr., C. E., and Vujnovic, B. J. (2002). The use of ultrasound for cleaning coal. In *Proceedings of the 19th Annual International Coal Preparation Exhibition and Conference*, volume 1, page 61–67. <http://web.archive.org/web/20190713150249if/http://www.bixbydental.com:80/about/news/coalultrasound.pdf>.
- Hoff, L. (2001). *Acoustic Characterization of Contrast Agents for Medical Ultrasound Imaging*. Springer Dordrecht. <https://doi.org/10.1007/978-94-017-0613-1>.
- Hoff, L., Sontum, P. C., and Hovem, J. M. (2000). Oscillations of polymeric microbubbles: Effect of the encapsulating shell. *The Journal of the Acoustical Society of America*, 107:2272–2280. <https://doi.org/10.1121/1.428557>.
- Hu, Z. (2013). Comparison of Gilmore-Akulichev equation and Rayleigh-Plesset equation on the rapetic ultrasound bubble cavitation. Master's thesis, Iowa State University. <https://doi.org/10.31274/etd-180810-3261>.
- Karmazin, V. V. and Karmazin, V. I. (2005). *Magnetic, electrical and special methods of mineral processing*. Publishing house MGTU.
- Kozubková, M., Rautová, J., and Bojko, M. (2012). Mathematical Model of Cavitation and Modelling of Fluid Flow in Cone. *Procedia Engineering*, 39:9–18. XI-IIth International Scientific and Engineering Conference "Hermetic Sealing, Vibration Reliability and Ecological Safety of Pump and Compressor Machinery" - "HERVICON-2011". <https://doi.org/10.1016/j.proeng.2012.07.002>.
- Mast, T. D., Souriau, L. P., Liu, D.-L. D., Tabei, M., Nachman, A. I., and Waag, R. C. (2001). A k-space method for large-scale models of wave propagation in tissue. *IEEE Transactions on Ultrasonics, Ferroelectrics, and Frequency Control*, 48(2):341–354. <https://doi.org/10.1109/58.911717>.
- Morkun, V. and Morkun, N. (2018). Estimation of the Crushed Ore Particles Density in the Pulp Flow Based on the Dynamic Effects of High-Energy Ultrasound.

- Archives of Acoustics*, 43(1):61–67. <https://doi.org/10.24425/118080>.
- Morkun, V., Morkun, N., and Pikilnyak, A. (2014). The adaptive control for intensity of ultrasonic influence on iron ore pulp. *Metallurgical and Mining Industry*, 6(6):8–11. [https://www.metaljournal.com.ua/assets/MMI\\_2014\\_6/2-MorkunPikilnyak.pdf](https://www.metaljournal.com.ua/assets/MMI_2014_6/2-MorkunPikilnyak.pdf).
- Morkun, V., Morkun, N., and Tron, V. (2015a). Distributed closed-loop control formation for technological line of iron ore raw materials beneficiation. *Metallurgical and Mining Industry*, 7(7):16–19. [https://www.metaljournal.com.ua/assets/Journal/english-edition/MMI\\_2015\\_7/003Vladimir%20Morkun%2016-19.pdf](https://www.metaljournal.com.ua/assets/Journal/english-edition/MMI_2015_7/003Vladimir%20Morkun%2016-19.pdf).
- Morkun, V., Morkun, N., and Tron, V. (2015b). Distributed control of ore beneficiation interrelated processes under parametric uncertainty. *Metallurgical and Mining Industry*, 7(8):18–21. [https://www.metaljournal.com.ua/assets/Journal/english-edition/MMI\\_2015\\_8/004Morkun.pdf](https://www.metaljournal.com.ua/assets/Journal/english-edition/MMI_2015_8/004Morkun.pdf).
- Morkun, V., Morkun, N., and Tron, V. (2015c). Model synthesis of nonlinear nonstationary dynamical systems in concentrating production using Volterra kernel transformation. *Metallurgical and Mining Industry*, 7(10):6–9. [https://www.metaljournal.com.ua/assets/Journal/english-edition/MMI\\_2015\\_10/001Morkun.pdf](https://www.metaljournal.com.ua/assets/Journal/english-edition/MMI_2015_10/001Morkun.pdf).
- Morkun, V., Semerikov, S., Hryshchenko, S., and Slovak, K. (2017). Environmental geo-information technologies as a tool of pre-service mining engineer's training for sustainable development of mining industry. In Ermolayev, V., Bassiliades, N., Fill, H., Yakovyna, V., Mayr, H. C., Kharchenko, V. S., Peschanenko, V. S., Shyshkina, M., Nikitchenko, M. S., and Spivakovsky, A., editors, *Proceedings of the 13th International Conference on ICT in Education, Research and Industrial Applications. Integration, Harmonization and Knowledge Transfer, ICTERI 2017, Kyiv, Ukraine, May 15-18, 2017*, volume 1844 of *CEUR Workshop Proceedings*, pages 303–310. CEUR-WS.org. <https://ceur-ws.org/Vol-1844/10000303.pdf>.
- Schnerr, G. H. and Sauer, J. (2001). Physical and Numerical Modeling of Unsteady Cavitation Dynamics. In *CMF-2001, 4th International Conference on Multiphase Flow. New Orleans, USA, May 27 - June 1, 2001*. <https://www.researchgate.net/publication/296196752>.
- Singhal, A. K., Athavale, M. M., Li, H., and Jiang, Y. (2002). Mathematical Basis and Validation of the Full Cavitation Model. *Journal of Fluids Engineering*, 124(3):617–624. <https://doi.org/10.1115/1.1486223>.
- Soneson, J. (2011). High intensity focused ultrasound simulator. <https://www.mathworks.com/matlabcentral/fileexchange/30886-high-intensity-focused-ultrasound-simulator>.
- Soyama, H. and Korsunsky, A. M. (2022). A critical comparative review of cavitation peening and other surface peening methods. *Journal of Materials Processing Technology*, 305:117586. <https://doi.org/10.1016/j.jmatprotec.2022.117586>.
- Tabei, M., Mast, T. D., and Waag, R. C. (2002). A k-space method for coupled first-order acoustic propagation equations. *The Journal of the Acoustical Society of America*, 111(1):53–63. <https://doi.org/10.1121/1.1421344>.
- Vlasko-Vlasov, V. K. and Tikhomirov, O. A. (1991). Oscillations of monopolar domain walls in the field of ultrasonic waves. *Solid State Physics*, 33(12):3498–3501. <https://journals.ioffe.ru/articles/22125>.